EFFECT OF THE ROUGHNESS OF THE INTERFACE ON DISSOLUTION OF GAS MOLECULES: THE CASE OF CO_2

A DISSERTATION REPORT

By

RAJAT PUNDHIR

DEPARTMENT OF CHEMISTRY
INDIAN INSTITUTE OF TECHNOLOGY ROORKEE
ROOKEE-247 667 (INDIA)
MAY, 2019

EFFECT OF THE ROUGHNESS OF THE INTERFACE ON DISSOLUTION OF GAS MOLECULES: THE CASE OF CO_2

A DISSERTATION REPORT

Submitted in partial fulfilment of the requirements for the award of the degree

of

MASTER OF TECHNOLOGY

in

ADVANCE CHEMICAL ANALYSIS

by

RAJAT PUNDHIR

DEPARTMENT OF CHEMISTRY
INDIAN INSTITUTE OF TECHNOLOGY ROORKEE
ROOKEE-247 667 (INDIA)
MAY, 2019

INDIAN INSTITUTE OF TECHNOLOGY ROORKEE
ROORKEE

CANDIDATE'S DECLARATION

I hereby certify that the work which is being presented in the thesis entitled **"EFFECT OF THE ROUGHNESS OF THE INTERFACE ON DISSOLUTION OF GAS MOLECULES: THE CASE OF CO_2"** in partial fulfilment of the requirements for the award of the Master of Technology and submitted in the Department of Chemistry of Indian Institute of Technology Roorkee, Roorkee is an authentic record of my own work carried out during a period from June, 2018 to May, 2019 under the supervision of Dr. C. N. Ramachandran, Assistant Professor, Department of Chemistry, Indian Institute of Technology Roorkee, Roorkee.

The matter presented in this dissertation report has not been submitted by me for the award of any other degree of this or any other institution.

(RAJAT PUNDHIR)

This is to certify that the above statement made by the candidate is correct to the best of my knowledge.

Dr. C. N. Ramachandran

(Supervisor)

Date:

ACKNOWLEDGEMENTS

I offer my sincerest gratitude and heartfelt thanks to my supervisor **Dr. C. N. Ramachandran**, whose guidance, encouragement and motivation during the course of the present study. I wholeheartedly acknowledge his full cooperation that I received from the very beginning of this work up to the completion in the form of this thesis.

I would like to express my gratitude towards **Prof. K.R. Justin Thomas**, HOD, Department of Chemistry, IIT Roorkee and **Prof. M.R. Maurya**, former HOD, Department of Chemistry, IIT Roorkee for their keen interest on me at every stage of my project.

I heartily thanks to **Mr. Sujit K. S**, for mentoring throughout the project work. I am also grateful to **Ms. Ankita Joshi** for their invaluable help during the project work. I am very thankful to **Mr. Vishal Kumar** for providing such a positive environment in lab.

I would also like to thank my lab seniors **Surinder Pal Kaur**, **Vinit Pundir**, **Mohan Tiwari**, **Peaush Gangwar**, **Angat Dhiman** and **Paras** for their constant support and help during the course of my project.

Without the selfless love, blessings and support of my loving parents, family, **Shubham**, **Divyani**, **Kavita**, friends and well-wishers, my efforts would be fruitless. Thank you to you all!

RAJAT PUNDHIR

IIT Roorkee

May 2019

CHAPTER 1

INTRODUCTION

The interface plays an important role in almost all fields of science including chemistry, physics, and engineering. In the field of surface chemistry, the physical and chemical phenomena are mainly studied at the interface. The interface is that region or boundary where two phases meet. The interface is very important in physical and chemical processes, as the atoms or molecules forming the surface or interface have different properties than those in the bulk due to different environment for both. The interfacial effect results in various applications like electro-catalysis, photo-catalysis, surface engineering, charge transfer, semiconductors, polymerization, bio-interface and many other critical processes.

In pharmaceutical industry, the drug has to pass through the interface for its pharmacological effect. The amount of dosage depends upon the way drug interacts with interface. The physical properties of composite material also depend upon the interface fractional volume. The stability and performance of solar cells can also be improved by understanding of different interfaces.

Different types of interfaces are:

i. Liquid – Gas interface
ii. Liquid – Liquid interface
iii. Solid – Liquid interface
iv. Solid – Gas interface

There is no interface between gases due to complete miscibility. The surface molecules of a liquid have higher energy than the molecules in the bulk. The bulk molecules have a similar kind of attraction from all the sides whereas the surface molecules have an absence of the neighboring molecules above them. This unbalanced force on the surface molecules gives rise to tension to the atoms known as surface tension. The other gas atoms or molecules attract towards the surface due to this unbalanced forces.

The process of accumulation of gas molecules at the surface of the liquid is termed as adsorption. The molecules which are adsorbed at the surface are called adsorbate and the surface at which molecules are adsorbed called adsorbent. In adsorption, the gas molecules are first adsorbed at the surface and then by overcoming the surface tension, these molecules are uniformly distributed in the bulk liquid.[1-5] The reverse process of adsorption, i.e removal of adsorbed molecules or atoms is known as desorption. In present work liquid gas interface is study due to its importance in the field of industry, biology, and atmospheric chemistry. During respiration the oxygen and carbon dioxide molecules from blood stream gets breathe in and out. In atmospheric chemistry, carbon dioxide gets dissolve in sea water resulting decrease of pH. The study of the interfacial phenomenon has a variety of application in petroleum industries including the separation of a mixture of hydrophilic solute molecules.[6] The interfacial phenomenon has an indirect application for gas hydrates in natural gas industries.

1.1 Literature survey

A molecular level understanding of the surface is important to understand the processes happening at the surface and this can be obtained by molecular dynamics simulation studies. The studies on the interface between water and gas molecules reported earlier[5,7,8] considered the surface as a slab neglecting the roughness of the interface.[3-5] The recent studies conducted on the water-methane interface by Sujith et al. considered the role of surface roughness. In a real system, the interface is not a planar surface instead it is a rough surface with several humps and wells.[9,10] The problem with the studies considering interface as a planar surface is that the molecules at the interface may be from the bulk phase or from the gas phase. Hence, the results reported while considering interface as planar surface are erroneous. In the present study, CO_2 gas is adsorbed on the surface of the water-methanol mixture. The interface also takes an important role in the formation of gas hydrates.[11-18] CO_2 is selected due to its important role in the extraction of CH_4 by a replacement mechanism using CO_2.[19-25] In this method, the CO_2 gas molecule in the gaseous or liquid form is injected to hydrate sediment. In liquid slab, methanol a hydrate inhibitor[26] is used with water.

The best feature of this replacement technique is sequestration of CO_2 gas that makes this technique environmental friendly as compared to other techniques of extraction of CH_4. Another advantage of this technique is CO_2 hydrate formation is an exothermic process and the heat released is sufficient for dissociation of CH_4 hydrate.[27] During the extraction process of gas hydrate, the surface dissociation takes place by various techniques including thermal stimulation, depressurization and inhibitor injection.[28-42] In contrast to the alternative extraction technique, the formation of CO_2 gas hydrate during the replacement method ensures the stability of the ocean sediment. The low temperature studies on gas hydrates suggested that CH_4 hydrate are thermodynamically less stable compared to CO_2 hydrate.[43] The molecular dynamic simulation studies supported the substitution of CH_4 molecules with CO_2 gas molecules inside the water cages[44,45].

In the present work, an algorithm similar to the algorithm suggested by Pártay et al.[46,47] and used earlier by Sujith et al.[9,10] is implemented to find the truly interfacial surface. To find the solvent molecules at the interface, a probe in the z-direction is moved as reported earlier.[9,10] By applying this method, all of the water-methanol molecules at the interface are identified.

1.2 Interfacial structure and dynamics: (Liquid-Gas)

The interfacial phenomenon like the dissolution of gas and formation of hydrate cannot be inferred without a deep understanding of the dynamic structure of the interface between liquid and gas.[48] The interface between liquid and gas plays a key role in the adsorption and dissolution of gases and is very important in the fundamental and application points of view. Among those gases, the interaction of methane and carbon dioxide with water is of utmost importance in gas hydrate nucleation, ultimately significant in atmospheric chemistry.[49] Earlier studies were focused solely on the interactions of gas molecules with pure water.[8] However, considering the role of methanol as a gas hydrate inhibitor, it is very important to study the interactions in the presence of a co-solvent such as methanol.[50] Experimental studies on the solubility of carbon dioxide (CO_2) in water-methanol mixture revealed that the solubility of the gases increases either by adding methanol in excess or by decreasing the temperature.[51]

There are two types of mechanisms reported in the literature on the dissolution of gases. In the first mechanism, the gas molecules enter into the bulk water with progressive hydration by the surface water molecules.[3] In the latter, gas molecules cross the liquid-gas interface by forming the cavities arising due to the density fluctuations in water.[5] However, the above mechanisms on the dissolution of gases through the interface into the bulk of water do not consider the effect of co-solvent at the liquid-gas interface. Although there are some studies available about the dissolution of methane in water both in the presence and absence of a co-solvent, not much is known about the dissolution of carbon dioxide; the gas that leads to global warming.[10] Considering the fact that experimental studies are difficult to perform to get insight at the molecular level, the present work based on molecular dynamic simulation is an attempt on the same.

1.3 Objectives of the Dissertation

The objective of the dissertation is to study the interfacial phenomenon of the interaction of gases like CO_2 and CH_4 with a liquid surface that is vital for understanding gas dissolution and hydrate nucleation. Some studies are reported on the structure and dynamics of water–gas interaction.[7] Still, the understanding of the interaction of gas molecules at the water-gas interface is inadequate to explain the processes like gas adsorption and dissolution. The goal of the dissertation is to study the interface between water and carbon dioxide gas especially the effect of methanol on the surface roughness of water-carbon dioxide system at the molecular level which was not reported in earlier studies.

In this study, the number density distribution of CO_2 molecules at humps and wells is studied with various concentration of methanol in water. The dissertation also aims on the understanding of the interface at the molecular level for the water-methanol mixture. Methanol is amphiphilic in nature which affects the characteristic properties of the water-methanol surface.[52-55] The interaction of a mixture of CO_2 and CH_4 on the water-methanol mixture is also studied. The competitive nature of CO_2 while adsorption and dissolution on the water-methanol surface instead of CH_4 is also analyzed in the present work.

1.4 Organization of Dissertation

An introduction about surfaces and a brief literature review of earlier studies on the interface, particularly the molecular level studies of the water-methanol mixture is summarized in **Chapter-I**.

In **Chapter-II** details about various models and theoretical aspects of computational methods used for the present study are given.

Chapter-III reports the density distribution of carbon dioxide at humps and wells corresponding to different fractions of methanol in water. The effect of methanol on interfacial surface tension and kinetic energy of the CO_2 at interface is examined. The effect of the gas hydrate inhibitor methanol on the surface roughness of the interface is presented. The difference between the number density of humps and wells is analyzed. The simulations are performed to determine the effect of CH_4 on the adsorption of CO_2. The effect of non-bonded interactions between C_{CO_2}-C_{CH_4}, C_{CH_4}-O_{H_2O}, C_{CO_2}- O_{H_2O}, C_{CH_4}-H_{H_2O} and C_{CO_2}-H_{H_2O} on the adsorption of carbon dioxide and methane mixture is studied. The entry of gas molecules from the interface and the effect of pressure is also examined for the mixture of CO_2 and CH_4 gases.

Chapter-IV concludes the important analysis of the present study and the future scope.

CHAPTER 2

COMPUTATIONAL METHODOLOGY

The present work aims on the investigation of the interfacial surface between water and gas molecules. To understand the structure and dynamics of the water-gas interface at molecular-level, molecular dynamics (MD) simulations are used in several studies.[4,5,56] Hence, molecular dynamics (MD) simulation techniques are employed in this study. A brief introduction to molecular dynamics and an outline of molecular models and various steps involved in the simulations are discussed below.

2.1 Molecular Dynamic Simulation

The development of technology leads to digitalization whether it is a day to day life activities or any kind of research. The development of research leads to use of fields like computational studies, complex algorithms, and various techniques. The computational techniques like molecular dynamic simulations made possible to study protein structures, physical and chemical properties of nanomaterial at the molecular level with respect to time. The position and velocity of molecules with respect to time is updated and to do so a deep knowledge about the interaction of forces on each atom and molecule during simulation steps is very important. On the basis of the force field calculation, the molecular dynamics technique is divided into two categories viz (i) classical molecular dynamics [57] and (ii) *ab initio* molecular dynamics (AIMD).[58]

In *ab initio* molecular dynamic techniques, the quantum mechanics concepts are used for force field calculation whereas in classical molecular technique Newtonian equations of motion and empirical potential equations are used for force field calculation. The *ab initio* molecular dynamics technique generates accurate forces at small time step but the issue is higher computational simulation cost and limitation of the number of atoms that can be used in the simulation.

In classical molecular dynamics (MD) simulation, the computational expense is less and the force field calculation associated with this technique guaranteed accurate quantum mechanical results for the simulation containing a large number of atoms.

The advantages like lesser computational cost, generating accurate force field and applicability to a large number of atoms made classical MD simulation to be our choice for the present study. MD simulation mimics the real system and helps to understand the molecular level details. Additionally, computer simulation is a good tool to replicate experimental results. The potential energy and various bonded and non-bonded interaction to atom and molecules at any instant are discussed below.

2.2 Empirical Force Field

The important step during simulation is to calculate a force field. The force field consists of two types of interaction energies, bonded and non-bonded.

2.2.1 Bonded Interaction

The bonded atoms include four types of interaction potential: stretching, bending, improper dihedral and proper dihedral. The interaction potential energy (V) consisting of bonds and angles are depicted by harmonic potential functions.

(a) Potential energy function

The bond stretching potential energy function (V_{str}) is given by

$$V_{str} = \frac{1}{2} k_{str} (r - r_o)^2 \quad 2.1$$

Where k_{str} is stretching force constant and (r-r_o) is the change in equilibrium bond length.

(b) Angle bending potential energy

The angle bending potential energy (V_{bend}) is given by

$$V_{bend} = \frac{1}{2} k_{bend} (\theta - \theta_o)^2 \quad 2.2$$

Where k_{bend} is the bending force constant and $(\theta - \theta_o)$ is the deviation from the equilibrium bond angle.

(c) Improper dihedral potential energy

The improper dihedral potential energy (V_{imp}) is given by

$$V_{imp} = \frac{1}{2} k_{imp} (\omega - \omega_o)^2 \quad 2.3$$

Where k_{imp} is force constant and $(\omega - \omega_o)$ is a change in optimal angle value.

(d) Proper dihedral potential energy

The proper potential energy (V_{pro}) is given by

$$V_{pro} = \frac{1}{2} k_{pro} \cos(n\varphi - \varphi_o) \quad 2.4$$

Where k_{pro} is rotational force constant, n corresponds to periodicity and the optimal value of the dihedral angle is represented as φ_o.

2.2.2 Non-Bonded Interaction

The bonded interactions between covalently bonded atoms or molecules are discussed above. Other than bonded interactions, there are interactions between non-covalently bonded atoms or molecules known as non-bonded interaction. This non-covalent interaction potential includes Lennard-Jones (L-J) potential and Coulombic potential.

(a) Lennard-Jones (L-J) potential

The van der Waals interaction between non-charged atoms is accounted for the Lennard-Jones potential energy function. The van der Waals interaction at an infinite interatomic distance (r) is zero. As the interatomic distance (r) decreases, the energy decreases and passes through minimum energy. On further decrease of interatomic distance (r), the energy goes up. The Lennard-Jones potential is defined as

$$V_{L-J} = 4\varepsilon[\left(\frac{\sigma}{r}\right)^{12} - \left(\frac{\sigma}{r}\right)^{6}] \quad 2.5$$

Where ε and σ are L-J parameters. σ is van der waals diameter and ε is the well depth.

In the above L-J potential function, the repulsive term, r^{-12} will be dominating at a small distance else the second term r^{-6} of L-J potential will be dominating which accounts for the attractive interactions.

(b) Coulombic Interactions

The interaction between charged ions or molecules is known as electrostatic or columbic interaction. The coulombic interactions V_c is expressed as

$$V_c = \frac{q_1 q_2}{4\pi\epsilon_o r_{12}} \quad 2.6$$

The columbic interactions are directly proportional to partial charges q_1 and q_2 and inversely proportional to ϵ_o and r_{12}, the dielectric constant and interatomic distance respectively.

The bonded and non-bonded interactions are considered in the force field used for the simulation. In the present study on the effect of roughness of the interface on the dissolution of gas molecules, water, carbon dioxide, and methanol molecules were represented by TIP4P[59], EPM2[60] and OPLS-UA[61,62] models, respectively. In this study, the force fields employed is OPLS.[63] As earlier studies reported[64] with this force field showed accurate results and compatibility of the above models.

2.3 Leap-Frog Algorithm

Integrating Newton's equation of motion are used for simulations starting with initial conditions. To know detailed dynamics such as motion of atoms in classical molecular dynamics the algorithm called "leapfrog" is used. In the leap-frog algorithm, the position and velocity leap over each other with the evolution of time. In the leap-frog algorithm, the position is calculated at constant time interval dt and velocities are calculated at a half time interval of position. The disadvantage of the leap-frog algorithm is that the position (X) and velocity (V) are updated half a time step, due to which exact velocity cannot be calculated at a position for the same time.

$$\frac{dX}{dt} = V \quad 2.7$$

$$\frac{-dU(X)}{dX} = \frac{dV}{dt} = F(X) \quad 2.8$$

Here, U(X) and F(X) are potential energy and force on particle when it is at position X and mass is assumed to be unity.

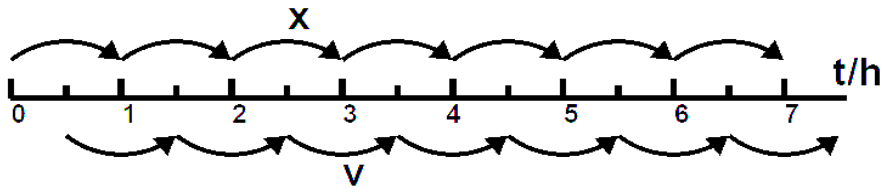

Figure 1: Leap Frog representation of position and velocity.

By applying Euler's method and midpoint method of approximation to equation 2.7 and 2.8, the general formulae for the leap-frog algorithm are

$$X_{n+1} = X_n + h\,V_{n+\frac{1}{2}} \tag{2.9}$$

$$V_{n+\frac{3}{2}} = V_{n+\frac{1}{2}} + h\,F(X_{n+1}) \tag{2.10}$$

2.4 Velocity Verlet Algorithm

The above discussed leap-frog algorithm is only useful when we have the starting velocity $V_{\frac{1}{2}}$ of the algorithm. As initial velocity V_o and initial position X_o are known, the leapfrog algorithm cannot proceed without calculating the value of $V_{\frac{1}{2}}$.

Thus, an approximation is done to Euler method in which instead of doing a full step for the Euler method, a single half step is performed for velocity calculation.

$$V_{\frac{1}{2}} = V_o + \frac{1}{2}\,h\,F(X_o) \tag{2.11}$$

As a result, velocity calculation is done in two equal half steps successively which are related to each other. This method of determination of position X and velocity V at the same time using the leapfrog algorithm is called velocity verlet.

$$V_{n+\frac{1}{2}} = V_n + \frac{1}{2}\,h\,F(X_n) \tag{2.12}$$

$$X_{n+1} = X_n + h\,V_{n+\frac{1}{2}} \tag{2.13}$$

$$V_{n+1} = V_{n+\frac{1}{2}} + \frac{1}{2}\,h\,F(X_{n+1}) \tag{2.14}$$

2.5 Types of Ensembles

In the present study, the widely used molecular dynamics simulation program GROMACS is used for all the calculations [65]. The thermodynamic properties like temperature and pressure are replicated with experimental processes to perform the molecular dynamic simulation. The MD simulation is performed in microcanonical (NVE) or in canonical (NVT) ensemble.

In the case of the NVE ensemble, the temperature and pressure are not constant. Thus, the position and velocity by Newton's equation of motion are not correct. Hence, resulting in an error in conservation of energy while performing simulations. Also, in NVE ensemble more precise position and velocity can be calculated by taking smaller time step during simulation which results in higher computational cost.

The canonical NVT ensemble, the temperature is maintained constant and NVT simulations are executed for a fixed number of atoms in a closed system. To maintain the temperature, the simulation system is coupled with thermostat, named as Nose-Hoover.[66-67] The temperature and pressure are kept constant throughout the simulation using the isothermal-isobaric (NPT) ensemble, where Parrinello-Rahman barostats [68] is coupled with Berendsen thermostat[69] for this purpose.

In this work both, NVT and NPT ensembles are performed for liquid slab simulations. The final energy minimization is performed followed by production simulation. Different steps performed in MD simulation are discussed below.

2.6 Simulation Procedure

The molecular dynamic simulation involves various steps viz. energy minimization, NVT ensemble, NPT ensemble and finally production simulation for 100 ns with a time step of 2fs. The interface between the methanol-water liquid mixture and carbon dioxide was simulated for 0.0, 0.1, 0.3, 0.5, 0.7, mole fraction of methanol in water. The simulation box of dimensions 4nm x 4nm x 20nm used for this purpose (Fig. 2) was divided into two parts; one containing a mixture of water and methanol keeping the total number of molecules as 4000 and the other containing carbon dioxide molecules maintain a pressure of 40 bar. The

interaction of CO_2 with pure water as well as that with various mole fractions of methanol in water is studied.

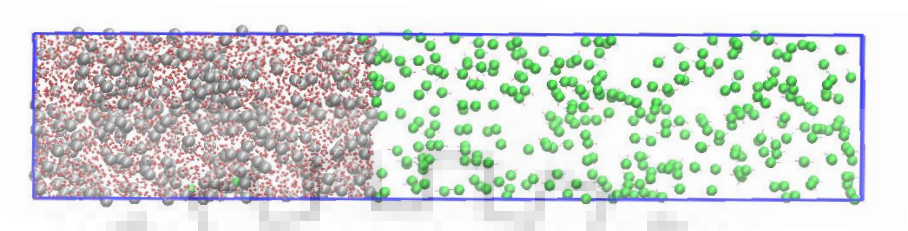

Figure 2: Initial simulation box of dimension 4nm x 4nm x 20nm system containing methanol (Grey), water (Red point) and CO_2 (Green) molecules

The numbers of particles are limited in molecular dynamics simulation. To overcome this problem the periodic boundary condition is applied in x, y, z, direction. In periodic boundary condition, the image of the simulation box is surrounded to itself which ensures that the system is continuous in all directions. The simulations were carried out at a temperature of 270 K and a pressure of 40 bar using the program GROMACS-4.6.5.[57] More details about the simulation are briefly discussed below.

2.6.1 Energy Minimization

The removal of unfavorable interactions of the initial simulation system between the atoms or molecules is done in energy minimization step. The energy minimization in molecular dynamic simulation is done according to the steepest descent method. In the steepest descent method, a critical value is set for maximum potential force as 1000 kJ mol^{-1} nm^{-1} for a system containing 2000 – 6000 water molecule and when simulation system reaches this maximum force of 1000 kJ mol^{-1} nm^{-1} the energy minimization step is successfully finished. The negative potential energy after energy minimization step should be in the order of 10^5-10^6 for the simulation system containing water.

2.6.2 NVT and NPT Ensemble

In the energy minimization step, the unfavorable interaction between atoms or molecules is removed from the initial simulation system. In the equilibration step, the desired temperature and pressure is achieved by a series of simulation. The NVT ensemble

simulations are performed to equilibrate the temperature to 270K and NPT ensemble simulations are performed to compress the liquid slab to a pressure of 40 bar. In this step Nose-Hoover[66,67] thermostat is coupled with Parrinello-Rahman barostat[68], where temperature and pressure are controlled, respectively. The NVT simulation is performed to bring the simulation system to the desired temperature whereas isothermal-isobaric NPT simulation is performed to bring the simulation system to the desired pressure. In NPT simulation the system is coupled to barostat for equilibrating pressure and simultaneously coupled with a thermostat to maintain the temperature of the simulation system.

2.6.3 Production Simulation

In this step, the well equilibrated simulated system from NVT-NPT ensemble is allowed to simulate for a sufficiently long time. The trajectory generated after the simulation is analyzed to get insight on the process after production simulation. The various properties like surface roughness and density distribution are studied with the help of trajectory generated. Detailed analysis and discussion of the results after production simulation are given below in chapter-3.

CHAPTER 3

RESULTS AND DISCUSSION

The earlier studies on the liquid-gas interface were reported only for the adsorption of methane gas (CH_4) and not much is known about the carbon dioxide adsorption.[1-3,10,53] Besides, there has been no conclusive understanding of the optimum amount of methanol required for surface roughness in previous studies.[9,10,46,50,51,55] In this chapter, we have examined the effect of methanol (CH_3OH) concentration on the surface roughness of the water-carbon dioxide (H_2O-CO_2) interface. The adsorption and dissolution of the gases such as CO_2 and CH_4 in their different composition on the methanol-water mixture are investigated and the results are analyzed. The compositions of CH_3OH, H_2O and CO_2 incorporated in the simulation system are listed in table 3.1.

3.1 Effect of methanol on interfacial surface tension

The water molecules present in the bulk experience similar interactions from all the sides while that present in the surface do not have balancing interactions among themselves. Different interaction forces for the molecules at the interface give rise to the surface tension. The average surface tension at the interface of methanol-water (CH_3OH-H_2O) mixture was analyzed and the results are listed in table 3.2. The average surface tension was obtained by Berendsen pressure coupling method as implemented in the program by calculating the difference between the normal and lateral pressure at the surface.[69] From the table, it can be seen that the average surface tension decreases as the concentration of methanol increases in the liquid slab. The methanol molecules favour the adsorption phenomenon and hence the surface tension shows a sharp decline. During the adsorption process, the gas molecules come close to the neighboring molecules of the interface resulting a decrease in surface tension. Further, addition of methanol on water weakens the interaction forces between them. The interaction energy between water molecules, methanol molecules and their mixture follows the trend: H_2O-H_2O > CH_3OH-H_2O > CH_3OH-CH_3OH. As can be seen from table 3.2, the system with minimum interaction energy has lowest value of surface tension and that with maximum interaction energy exhibits the highest surface tension value. Thus, methanol

favours the adsorption as well as dissolution of carbon dioxide suggesting that the gas molecules can easily penetrates the liquid-gas interface in the presence of methanol.

Table 3.1 Composition of CH_3OH, H_2O and CO_2 in the simulation box of dimension 4 nm × 4 nm × 20 nm.

Mole fraction of CH_3OH	Number of CH_3OH	Number of H_2O	Number of CO_2
0	0	4000	330
0.1	400	3600	330
0.3	1200	2800	258
0.5	2000	2000	212
0.7	2800	1200	159

Table 3.2 The average value of surface tension corresponding to different mole fractions of CH_3OH in the liquid slab.

Mole fraction of CH_3OH	Average surface tension (bar nm)
0	924
0.1	637
0.3	467
0.5	433
0.7	417

3.2 Effect of methanol on kinetic energy of carbon dioxide at interface

Table 3.3 lists the values of kinetic energy of carbon dioxide molecules present in the gas slab corresponding to the different mole fractions of methanol. It can be seen clearly from the table that the kinetic energy of CO_2 molecules decreases on increasing the amount of methanol which is also reflected from the values of average surface tension listed in table 3.2. It is well-known that the velocity of a molecule is a key factor in determining its kinetic energy. The values of velocity were obtained via verlet algorithm as implemented in the program.[70]

Table 3.3 The average kinetic energy of CO_2 molecules corresponding to different mole fractions of CH_3OH molecules.

Mole fraction of CH_3OH	Average kinetic energy of CO_2 (kJ mol^{-1})
0.0	28788
0.1	28619
0.3	28384
0.5	28126
0.7	27828

3.3 Analysis of the number density of carbon dioxide at interface

Figure 3.1 shows the number density plots for the distribution of carbon dioxide at humps and wells corresponding to different mole fractions of methanol. The interface molecules are classified as in humps and in wells with respect to the average surface of the liquid. The position of the surface of the liquid was determined by averaging the z-coordinates of the molecules at the interface. In figure 3.1, the average surface of the liquid is at zero of distance and the liquid region left to the surface is taken as negative and the gas region at the right is considered as positive. The interface molecules were considered to be on the hump when the distance from the center of the liquid slab to these molecules is more than the distance to the average surface of the liquid. In contrast, the interfacial molecules on the well were those for which the distance from the center of the liquid slab is less than the corresponding distance to the average surface of the liquid. The number density of CO_2 at humps and wells was obtained by moving the probe in the z-direction. The probe while moving counts the number of CO_2 molecules in each segment. By repeating this procedure, the average number density profile of CO_2 at humps and wells was determined.

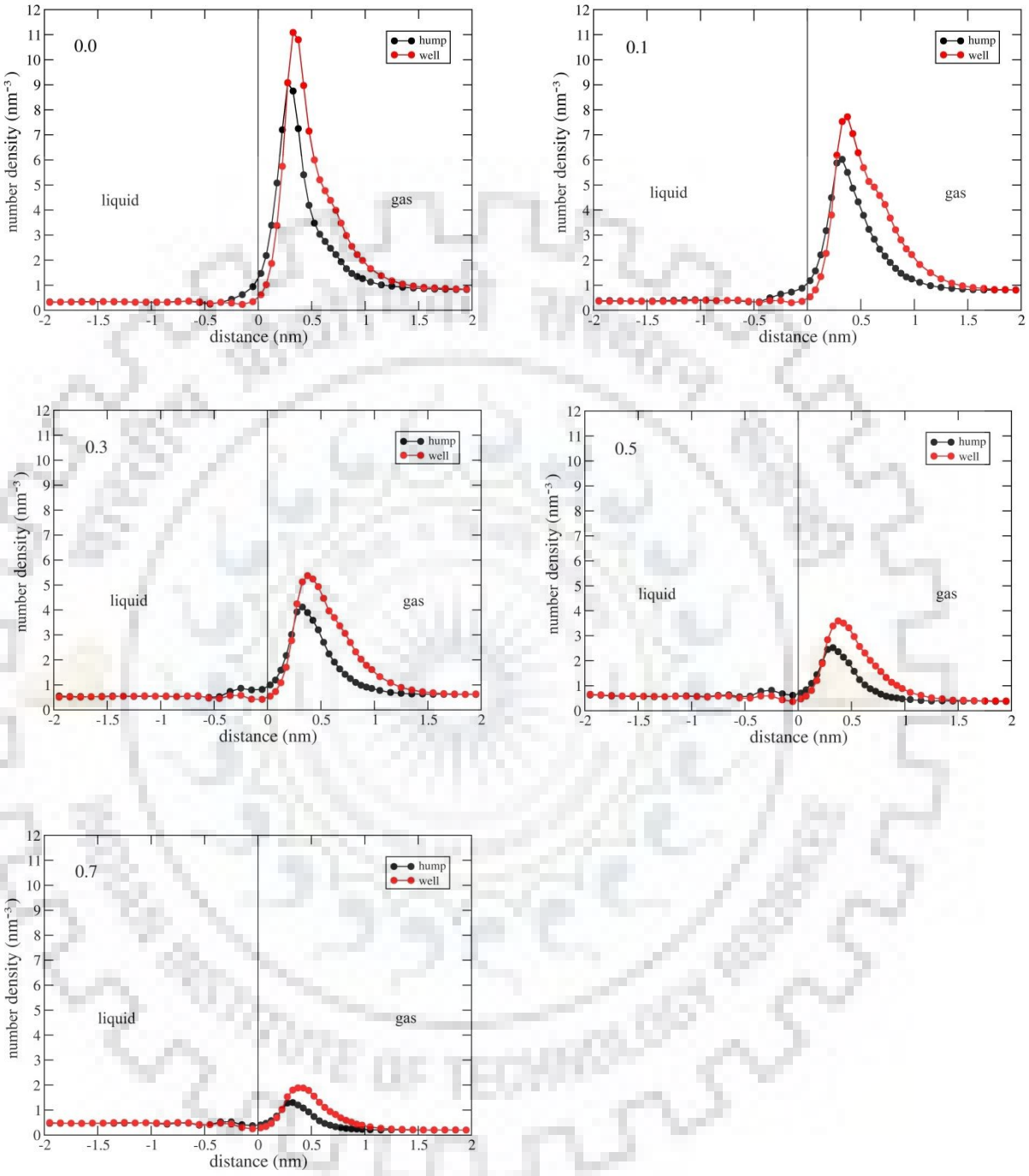

Figure 3.1 Number density plots of carbon dioxide corresponding to wells and humps for different mole fraction of methanol (0.0, 0.1, 0.3, 0.5, 0.7) in the surface of water-methanol mixture.

The region between 0.5 nm beneath the average liquid surface and 0.3 nm above the average liquid surface is referred to as the 'surface region'. The region between 0.3 nm to 1.5

nm above the surface is termed as ‘local region’ for further discussion. In the local region, CO_2 is accumulated near the surface, however, not in direct contact with the surface molecules. In the region beyond 1.5 nm above the liquid surface, no increment in the density of CO_2 is observed. The more density of CO_2 above humps and wells especially in the local region is due to non-bonded interactions between CO_2 and methanol-water mixture. As seen in figure 3.1, the key observation is the 'surface region' in which the number density of CO_2 is higher near the humps as compared to that near the wells. In contrast to this, the number density of CO_2 in the local region from 0.3 nm to 1.5 nm is higher near the wells. The higher density of CO_2 in humps in ‘surface region’ indicates that a higher probability of CO_2 to enter the bulk liquid region through humps. Humps act as preferred channels in comparison to wells for the entry of CO_2 into the bulk liquid.

3.4 Analysis of Surface Roughness

The interfacial surface roughness was examined to understand the impact of the roughness on the distribution of carbon dioxide at humps and wells of the liquid surface. The effect of methanol concentration on the surface roughness was also analyzed. Quantitative analysis of surface roughness is done in terms of the height of the humps and depth of the wells (which refers to amplitude α) and the closeness of humps or wells (which is referred to frequency γ). The horizontal separation (R) between surface solvent molecules and the vertical separation (S) between two molecules on the average surface is calculated using the formulae as used earlier.[71,72]

$$\boldsymbol{R} = \frac{\alpha\gamma S}{\alpha + \gamma S}$$

The variation of R versus S for various compositions is plotted in figure 3.2. It is evident from the figure that for a small value of S, the value of R increases linearly and becomes flat for larger values. The result indicates that with an increase in methanol concentration, the surface becomes rougher in terms of height and depth of humps and wells, respectively. The surface roughness increases and levels off for 0.1, 0.3, 0.5, and 0.7 mole fractions of methanol.

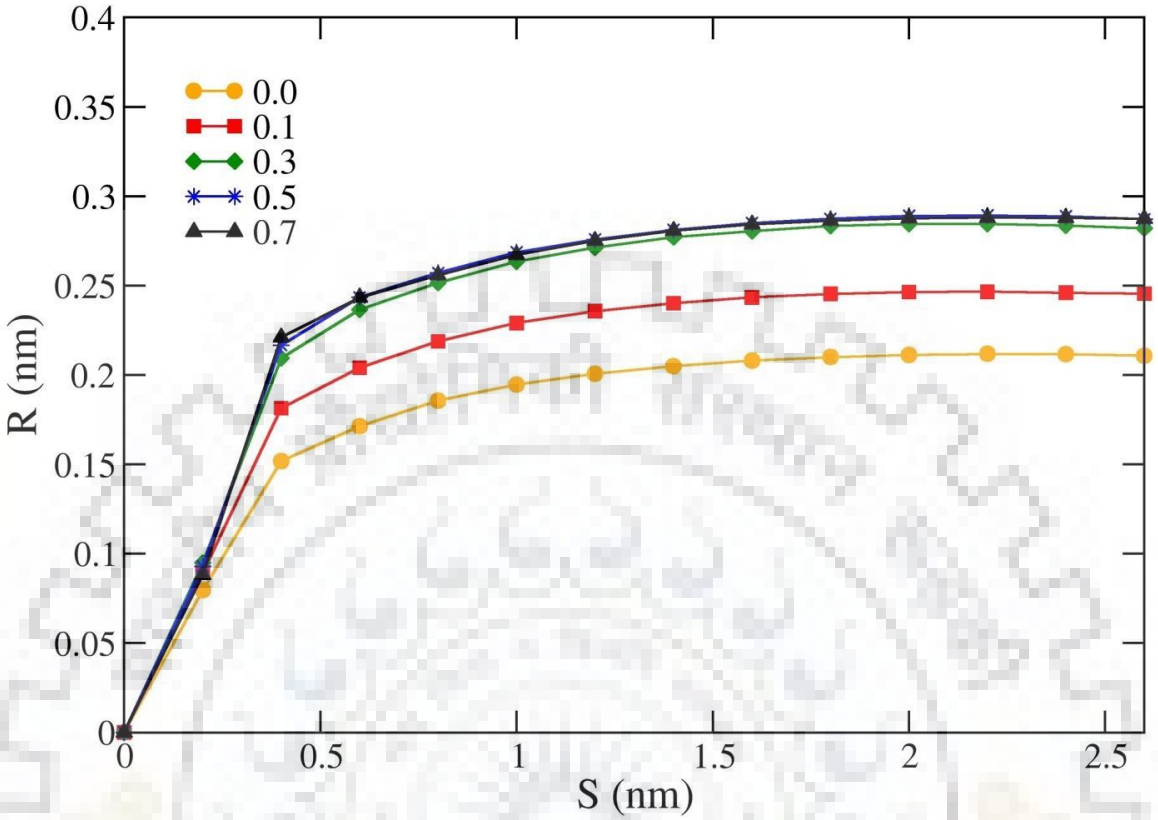

Figure 3.2 Horizontal separation (S) and vertical separation (R) between surface solvent molecules for various methanol mole fractions 0.0, 0.1, 0.3, 0.5, 0.7.

On comparing the surface roughness for 0.5 and 0.7 mole fractions of methanol, it can be inferred that the interface has become saturated in terms of roughness for 0.5 mole fraction of methanol. Thus, the optimum mole fraction of methanol at which the water-methanol surface has maximum roughness is 0.5. At this mole fraction, the maximum adsorption of carbon dioxide molecules takes place on the surface of methanol-water mixture.

3.5 Difference between the density of humps and wells ($d_{hump} - d_{well}$)

The number density of carbon dioxide on humps and wells was examined with respect to the distance for a better understanding of the distribution of carbon dioxide at the interface of the methanol-water mixture. The difference between the density of humps and

wells was calculated at various distances from the interface. Corresponding to the different mole fractions of methanol, the differences in the number density of humps and wells (d_{hump} – d_{well}) at various distances were plotted and are shown in figure 3.3.

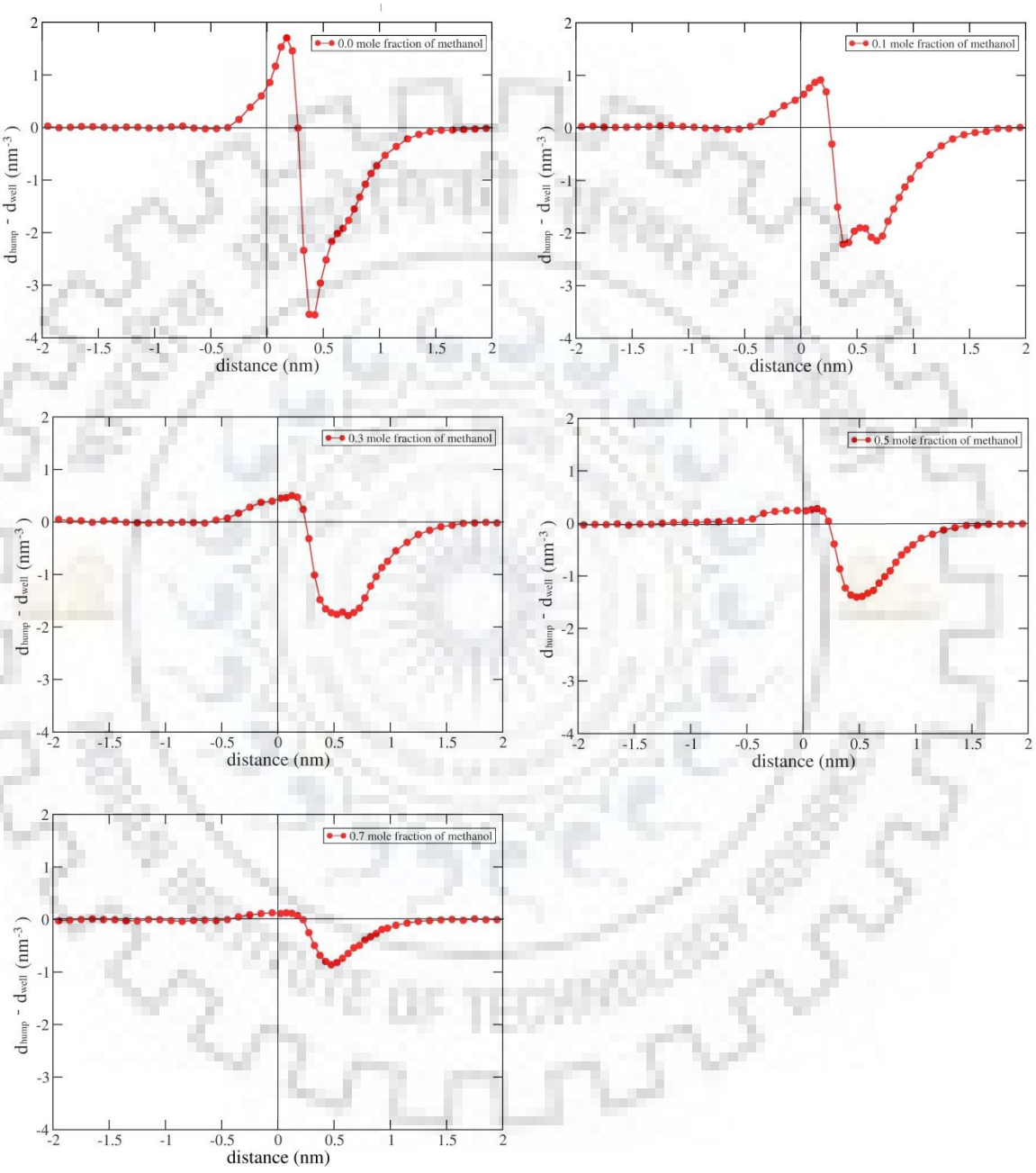

Figure 3.3 Difference in the number density of CO_2 molecules between humps and wells (d_{hump} - d_{well}) for 0.0, 0.1, 0.3, 0.5 and 0.7 mole fractions of methanol.

The number density difference ($d_{hump} - d_{well}$) is zero in the liquid region (< -0.5 nm) and (> 1.5 nm) in the gas region. The difference ($d_{hump} - d_{well}$) is positive in the surface region from 0.5 nm below and 0.3 nm above the liquid surface. In this region, there are more CO_2 molecules on the humps than the wells imply that the former is preferred channel for the entry of CO_2 molecules to the liquid region. The ($d_{hump} - d_{well}$) is negative in the local region (> 0.3 nm to < 1.5 nm) which indicates that there are more CO_2 molecules above the wells compared to the humps. The more number of CO_2 above the well could be due to the less width of the wells formed. However, this needs further studies and could not be investigated due to the dynamic behavior of the system.

3.6 Analysis of mixture of CH_4 and CO_2

The adsorption and dissolution of CO_2 in the presence of CH_4 on methanol-water interface were studied for 0.1 mole fraction of methanol (X_{CH_3OH}). The details about the composition of the simulation system are provided in table 3.4. The molecular dynamics simulations were performed to analyze the combined effect of both the gases (CO_2 and CH_4) on adsorption and dissolution. As mentioned in chapter-2, there are different force fields based on interaction energies. The bonded interaction includes four types of potential: stretching, bending, improper dihedral and proper dihedral. Whereas the non-bonded interaction includes Lennard-Jones (L-J) potential and Coulombic potential. The non-bonded parameters for the interactions between different types of molecules considered in this study are listed in table 3.5. The non-bonded interactions are considered between these atoms of molecule C_{CO_2}-C_{CH_4}, C_{CH_4}-O_{H_2O}, C_{CO_2}- O_{H_2O}, C_{CH_4}-H_{H_2O} and C_{CO_2}-H_{H_2O}.

Table 3.4 Compositions of various systems in the simulation box of dimension 4 nm × 4 nm × 20 nm.

X_{CH_3OH}	number of CH_3OH	number of H_2O	number of CO_2	number of CH_4
0.0	0	4000	130	130
0.1	400	3600	123	123

Table 3.5 The parameters used for C_{CO_2}-C_{CH_4}, C_{CH_4}-O_{H_2O}, C_{CO_2}- O_{H_2O}, C_{CH_4}-H_{H_2O} and C_{CO_2}-H_{H_2O}

i	J	Sigma (σ)	Epsilon (ε)
C_{CO_2}	C_{CH_4}	0.2892	0.3955
C_{CH_4}	O_{H_2O}	0.3116	0.2930
C_{CO_2}	O_{H_2O}	0.3030	0.5320
C_{CH_4}	H_{H_2O}	0.2814	0.3000
C_{CO_2}	H_{H_2O}	0.2194	0.3920

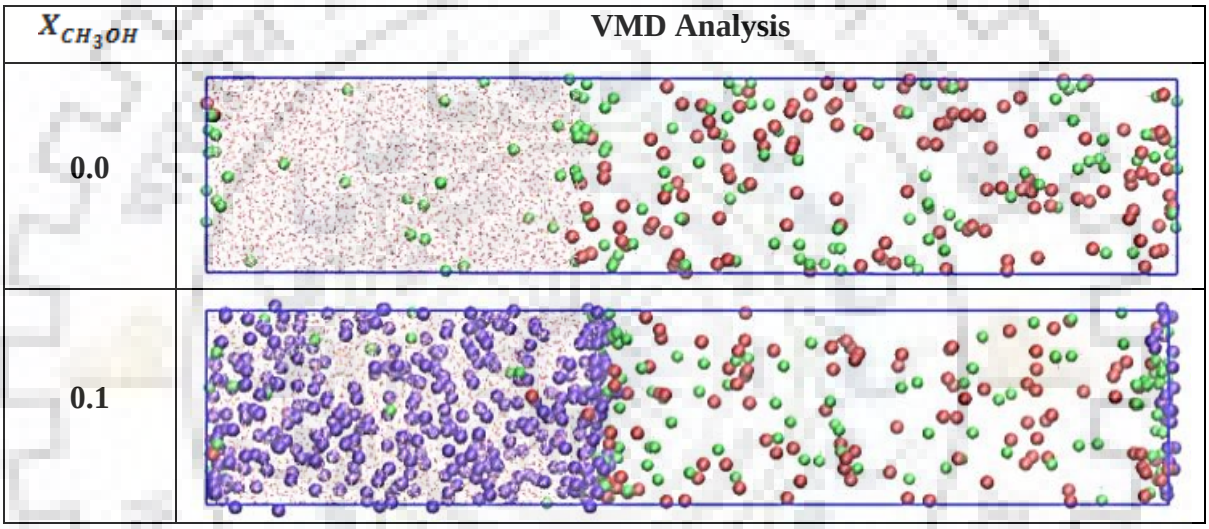

Figure 3.4 Simulation box of dimension 4 nm × 4 nm × 20 nm containing methanol (violet), water (O-red and H-white), CO_2 (green) and CH_4 (red) molecules.

The simulation systems with non-bonded interactions were visualized using the visual molecular dynamics (VMD) program[73] and are shown in figure 3.4. The effect of above interactions on the distribution of methane in liquid slab was analyzed from the above figure. It can be seen from the figure that the methane molecules are not entering into the liquid slab, irrespective of the methanol concentration and the interactions between the molecules. This can be explained based on the solubility of methane which does not change on adding methanol to the system.

3.7 Effect of pressure on CH_4 adsorption

The adsorption and dissolution of CH_4 on liquid slab was studied at a pressure of 50 bar for mixture of CO_2 and CH_4 gases. The compositions of the simulation systems are given in table 3.6. In the simulation box, the numbers of CH4 molecules are higher than that of CO_2 molecules. The simulation box for the system comprised of H_2O, CO_2 and CH_4 is shown in figure 3.5. It can be seen clearly from the figure that methane molecules are not entering the liquid slab. Thus, the increase in the pressure has no effect on the adsorption as well as the dissolution of CH_4 gas in the liquid slab. This is due much higher solubility of CO_2 than CH_4 gas.

Table 3.6 Compositions of the simulation systems (H_2O, CO_2 and CH_4) of dimension 4 nm × 4 nm × 20 nm.

number of H_2O	number of CO_2	number of CH_4
4000	70	165

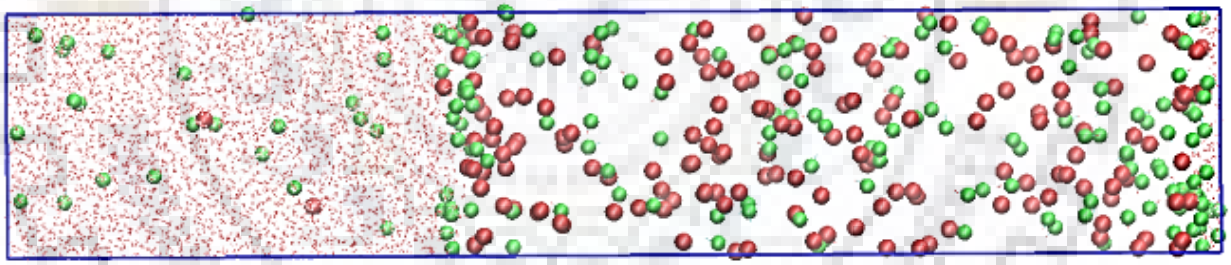

Figure 3.5 Simulation box of dimension 4 nm × 4 nm × 20 nm containing water (O-red and H-white), CO_2 (green) and CH_4 (red) molecules.

CHAPTER 4

CONCLUSION AND FUTURE SCOPE

In the present work adsorption and dissolution of the greenhouse gases carbon dioxide (CO_2) and methane (CH_4) is studied by performing classical molecular dynamics simulations. Simulation studies done on water – carbon dioxide interface provided insight on the effect of roughness of the interface on adsorption of carbon dioxide. The study shows that surface tension and kinetic energy decrease as methanol concentration increases in water. The effect of methanol was also studied which showed that an increase in concentration of methanol leads to more roughness of the surface which leads to larger humps. Analysis revealed that methanol facilitates the dissolution of carbon dioxide. The optimum concentration of methanol required is found to be 0.5 mole fraction for maximum surface roughness of the interface. The density distribution analysis and number density difference between humps and wells showed that the humps are preferred channels for carbon dioxide dissolution. The simulation studies are performed on mixture of CO_2 and CH_4 gas and results are examined by visual molecular dynamics (VMD) program, which infer that CH_4 molecules are not entering the liquid slab. This is due to lower solubility of methane than that of carbon dioxide. Further studies are necessary to understand that why the number density of CO_2 molecules is more above the wells in the local region. The probable reason could be due to the less width of the wells formed and can be investigated further. The above studies can be extended to other gas hydrate inhibitors in water slab. Considering the importance of present study in gas separation the above studies can also be extended for different liquid-gas interfaces.

References

1. R. Vacha, P. Slaviček, M. Mucha, B. J. Finlayson-Pitts, P. Jungwirth. Adsorption of Atmospherically Relevant Gases at the Air/Water Interface: Free Energy Profiles of Aqueous Solvation of N_2, O_2, O_3, OH, H_2O, HO_2 and H_2O_2. J. Phys. Chem. A, **2004**, 108, 11573-11579.
2. R. Vacha, P. Jungwirth, J. Chen, K. Valsaraj. Adsorption of Polycyclic Aromatic Hydrocarbons at the Air-Water Interface: Molecular Dynamics Simulations and Experimental Atmospheric Observations. Phys. Chem. Chem. Phys. , **2006**, 8, 4461-4467.
3. A. Ghoufi, P. Malfreyt. Numerical Evidence of the Formation of a Thin Microscopic Film of Methane at the Water Surface: A Free Energy Calculation. Phys. Chem. Chem. Phys. , **2010**, 12, 5203-5205.
4. T. Somasundaram, R. M. Lynden-Bell, C. H. Patterson. The Passage of Gases through the Liquid Water/Vapour Interface: A Simulation Study. Phys. Chem. Chem. Phys. , **1999**, 1, 143-148.
5. E. L. Murina, C. Pastorino, R. Fernandez-Prini. Entrance Dynamics of CH_4 Molecules through a Methane-Water Interface. Chem. Phys. Lett. , **2015**, 637, 13-17.
6. M. Sayou, R. Ishizuka, N. Matubayasi. Energetic Analysis of Adsorption and Absorption of Small Molecule to Nanodroplet of Water. J. Phys. Chem. B, **2017**, 121, 5995-6001.
7. S. K. Reed, R. E. Westacott. The Interface Between Water and a Hydrophobic Gas. Phys. Chem. Chem. Phys. , **2008**, 10, 4614-4622.
8. R. Sakamaki, A. K. Sum, T. Narumi, R. Ohmura, K. Yasuoka. Thermodynamic Properties of Methane/Water Interface Predicted by Molecular Dynamics Simulations. J. Chem. Phys. , **2011**, 134, 144702.
9. K.S. Sujith, C.N. Ramachandran. Effect of surface roughness on adsorption and distribution of methane atthe water-methane interface. Journal of Molecular Liquids, **2018**, 266, 856–863.
10. K.S. Sujith, Km Suman Lata, C.N. Ramachandran. Adsorption and dissolution of methane at the surface of the methanol-water mixture. Fluid Phase equilibria, **2018**, 473, 310-317.

11. H. Ueno, H. Akiba, S. Akatsu, R. Ohmura. Crystal Growth of Clathrate Hydrates Formed with Methane + Carbon Dioxide Mixed Gas at the Gas/Liquid Interface and in Liquid Water. New J. Chem. , **2015**, 39, 8254-8262.
12. J. D. Lee, M. Song, R. Susilo, P. Englezos. Dynamics of Methane-Propane Clathrate Hydrate Crystal Growth from Liquid Water with or without the Presence of n-Heptane. Cryst. Growth Des. , **2006**, 6, 1428-1439.
13. T. Koga, J. Wong, M. K. Endoh, D. Mahajan, C. Gutt, S. K. Satija. Hydrate Formation at the Methane/Water Interface on the Molecular Scale. Langmuir, **2010**, 26, 4627-4630.
14. T. Kodama, R. Ohmura. Crystal Growth of Clathrate Hydrate in Liquid Water in Contact with Methane + Ethane + Propane Gas Mixture. J. Chem. Technol. Biotechnol. , **2014**, 89, 1982-1986.
15. J. P. Long, E. D. Sloan. Hydrates in the Ocean and Evidence for the Location of Hydrate Formation. Int. J. Thermophys. , **1996**, 17, 1-13.
16. S. Watanabe, K. Saito, R. Ohmura. Crystal Growth of Clathrate Hydrate in Liquid Water Saturated with a Simulated Natural Gas. Cryst. Growth Des. , **2011**, 11, 3235-3242.
17. S. L. Li, C. Y. Sun, B. Liu, X. J. Feng, F. G. Li, L. T. Chen, G. J. Chen. Initial Thickness Measurements and Insights into Crystal Growth of Methane Hydrate Film. AIChE J. , **2013**, 59, 2145-2154.
18. S. Li, C. Sun, B. Liu, Z. Li, G. Chen, A. K. Sum. New Observations and Insights into the Morphology and Growth Kinetics of Hydrate Films. Sci. Rep. , **2014**, 4, 1.
19. M. Ota, T. Saito, T. Aida, M. Watanabe, Y. Sato, R. L. Smith, H. Inomata. Macro and Microscopic CH_4-CO_2 Replacement in CH_4 Hydrate Under Pressurized CO_2. AIChE J. , **2007**, 53, 2715-2721.
20. X. Zhou, S. Fan, D. Liang, J. Du. Replacement of Methane from Quartz Sand-Bearing Hydrate with Carbon Dioxide-in-Water Emulsion. Energy & Fuels, **2008**, 22, 1759-1764.
21. J. W. Jung, D. N. Espinoza, J. C. Santamarina. Properties and Phenomena Relevant to CH_4-CO_2 Replacement in Hydrate-Bearing Sediments. J. Geophys. Res. , **2010**, 115, B10102.

22. Y. Seo, S. Lee, J. Lee. Experimental Verification of Methane Replacement in Gas Hydrates by Carbon Dioxide. Chem. Eng. Trans. , **2013**, 32, 163-168.
23. J. Zhao, K. Xu, Y. Song, W. Liu, W. Lam, Y. Liu, K. Xue, Y. Zhu, X. Yu, Q. Li. A Review on Research on Replacement of CH_4 in Natural Gas Hydrates by Use of CO_2. Energies, **2012**, 5, 399-419.
24. M. Ota, K. Morohashi, Y. Abe, M. Watanabe, R. L. J. Smith, H. Inomata. Replacement of CH_4 in the Hydrate by Use of Liquid CO_2. Energy Convers. Manage. , **2005**, 46, 1680-1691.
25. S. Lee, Y. Lee, J. Lee, H. Lee, Y. Seo. Experimental Verification of Methane-Carbon Dioxide Replacement in Natural Gas Hydrates Using a Differential Scanning Calorimeter. Environ. Sci. Technol. , **2013**, 47, 13184-13190.
26. T. Yagasaki, M. Matsumoto, H. Tanaka. Effects of Thermodynamic Inhibitors on the Dissociation of Methane Hydrate: A Molecular Dynamics Study. Phys. Chem. Chem. Phys. , **2015**, 17, 32347-32357.
27. N. Goel. In situ Methane Hydrate Dissociation with Carbon Dioxide Sequestration: Current Knowledge and Issues. J. Pet. Sci. Eng. , **2006**, 51, 169-184.
28. Z. R. Chong, S. H. B. Yang, P. Babu, P. Linga, X. S. Li. Review of Natural Gas Hydrates as an Energy Resource: Prospects and Challenges. Appl. Energy, **2016**, 162, 1633-1652.
29. L. G. Tang, R. Xiao, C. Huang, Z. P. Feng, S. S. Fan. Experimental Investigation of Production Behavior of Gas Hydrate under Thermal Stimulation in Unconsolidated Sediment. Energy Fuels, **2005**, 19, 2402-2407.
30. W. X. Pang, W. Y. Xu, C. Y. Sun, C. L. Zhang, G. J. Chen. Methane Hydrate Dissociation Experiment in a Middle-sized Quiescent Reactor using Thermal Method. Fuel, **2009**, 88, 497-503.
31. D. L. Li, D. Q. Liang, S. S. Fan, X. S. Li, L. G. Tang, N. S. Huang. In situ Hydrate Dissociation using Microwave Heating: Preliminary Study. Energy Convers. Manage. , **2008**, 49, 2207-2213.
32. H. O. Kono, S. Narasimhan, F. Song, D. H. Smith. Synthesis of Methane Gas Hydrate in Porous Sediments and its Dissociation by Depressurizing. Powder Technol. , **2002**, 122, 239-246.

33. B. Li, X. S. Li, G. Li, J. C. Feng, Y. Wang. Depressurization Induced Gas Production from Hydrate Deposits with Low Gas Saturation in a Pilot-Scale Hydrate Simulator. Appl. Energy, 129, **2014**, 274-286.
34. F. Dong, X. Zang, D. Li, S. Fan, D. Liang. Experimental Investigation on Propane Hydrate Dissociation by High Concentration Methanol and Ethylene Glycol Solution Injection. Energy Fuels, **2009**, 23, 1563-1567.
35. S. Fan, Y. Zhang, G. Tian, D. Liang, D. Li. Natural Gas Hydrate Dissociation by Presence of Ethylene Glycol. Energy Fuels, **2006**, 20, 324-326.
36. J. Zhao, C. Cheng, Y. Song, W. Liu, Y. Liu, K. Xue, Z. Zhu, Z. Yang, D. Wang, M. Yang. Heat Transfer Analysis of Methane Hydrate Sediment Dissociation in a Closed Reactor by a Thermal Method. Energies, **2012**, 5, 1292-1308.
37. J. Zhao, D. Liu, M. Yang, Y. Song. Analysis of Heat Transfer Effects on Gas Production from Methane Hydrate by Depressurization. Int. J. Heat Mass Transfer, **2014**, 77, 529-541.
38. J. Zhao, J. Wang, W. Liu, Y. Song. Analysis of Heat Transfer Effects on Gas Production from Methane Hydrate by Thermal Stimulation. Int. J. Heat Mass Transfer, **2015**, 87, 145-150.
39. H. Oyama, Y. Konno, Y. Masuda, H. Narita. Dependence of Depressurization-Induced Dissociation of Methane Hydrate Bearing Laboratory Cores on Heat Transfer. Energy Fuels, 23, **2009**, 4995-5002.
40. J. Zhao, Z. Zhu, Y. Song, W. Liu, Y. Zhang, D. Wang. Analyzing the Process of Gas Production for Natural Gas Hydrate using Depressurization. Appl. Energy. , **2015**, 142, 125-134.
41. J. Lee, S. Park, W. Sung. An Experimental Study on the Productivity of Dissociated Gas from Gas Hydrate by Depressurization Scheme. Energy Convers. Manage. , **2010**, 51, 2510-2515.
42. X. Yang, C. Y. Sun, K. H. Su, Q. Yuan, Q. P. Li, G. J. Chen. A Three-Dimensional Study on the Formation and Dissociation of Methane Hydrate in Porous Sediment by Depressurization. Energy Convers. Manage. , **2012**, 56, 1-7.

43. K. Ohgaki, K. Takano, H. Sangawa, T. Matsubara, S. Nakano. Methane Exploitation by Carbon Dioxide from Gas Hydrates-Phase Equilibria for CO_2-CH_4 Mixed Hydrate System. J. Chem. Eng. Jpn. , **1996**, 29, 478-483.
44. E. M. Yezdimer, P. T. Cummings, A. A. Chialvo. Determination of the Gibbs Free Energy of Gas Replacement in SI Clathrate Hydrates by Molecular Simulation. J. Phys. Chem. A, **2002**, 106, 7982-7987.
45. S. Alavi, T. K. Woo. How much Carbon Dioxide can be Stored in the Structure H Clathrate Hydrates: A Molecular Dynamics Study. J. Chem. Phys. , **2007**, 126, 044703.
46. L. B. Pártay, P. Jedlovszky, A. Vincze, G. Horvai. Properties of Free Surface of Water-Methanol Mixtures. Analysis of the Truly Interfacial Molecular Layer in Computer Simulation. J. Phys. Chem. B, **2008**, 112, 5428-5438.
47. L. B. Pártay, G. Hantal, P. Jedlovszky, A. Vincze, G. Horvai. A New Method for Determining the Interfacial Molecules and Characterizing the Surface Roughness in Computer Simulations. Application to the Liquid-Vapor Interface of Water. J. Comput. Chem. , **2008**, 29, 945-956.
48. L. F. Phillips. Processes at the Gas-Liquid Interface. Int. Rev. Phys. Chem. , **2011**, 30, 301-333.
49. (a) D. Bai, G. Chen, X. Zhang, A.K. Sum, W. Wang. How Properties of Solid Surfaces Modulate the Nucleation of Gas Hydrate. Sci Rep **2015**, 5, 12747, (b) A. Y. Galashev, Atomistic simulations of methane interactions with an atmospheric moisture. J Chem Phys **2013**, 139 (12), 124303, (c) C. D. Ruppel, J. D. Kessler. The interaction of climate change and methane hydrates. Reviews of Geophysics. **2017**, 55 (1), 126-168.
50. S. Porgar, S.Saleh. Fekr, M. Ghiassai, B. Hashemi Hosseini, Methanol and sodium chloride inhibitors impact on carbon dioxide hydrate formation, South African Journal of Chemical Engineering, **2018**, 26, 1-10.
51. N. Schüler, K. Hecht, M. Kraut, R. Dittmeyer. On the Solubility of Carbon Dioxide in Binary Water–Methanol Mixtures. Journal of Chemical & Engineering Data. **2012**, 57 (8), 2304-2308.
52. T. M. Chang, L. X. Dang. Liquid-Vapor Interface of Methanol-Water Mixtures: A Molecular Dynamics Study. J. Phys. Chem. B. , **2005**, 109, 5759-5765.

53. H. Chen, W. Gan, R. Lu, Y. Guo, H. F. Wang. Determination of Structure and Energetics for Gibbs Surface Adsorption Layers of Binary Liquid Mixture 2. Methanol + Water. J. Phys. Chem. , **2005** B, 109, 8064-8075.
54. J. Sung, K. Park, D. Kim. Surfaces of Alcohol-Water Mixtures Studied by Sum-Frequency Generation Vibrational Spectroscopy. J. Phys. Chem. B, **2005**, 109, 18507-18514.
55. J. R. Choudhuri, A. Chandra. Hydrogen Bonded Structure, Polarity, Molecular Motion and Frequency Fluctuations at Liquid-Vapor Interface of a Water-Methanol Mixture: An Ab initio Molecular Dynamics Study. J. Chem. Phys. , **2014**, 141, 134703.
56. C. J. H. Knox, L. F. Phillips. Capillary-Wave Model of Gas-Liquid Exchange. J. Phys. Chem. B, **1998**, 102, 8469-8472.
57. D. van der Spoel, E. Lindahl, B. Hess, and the GROMACS development team, GROMACS User Manual version 4.6.5, www.gromacs.org, **2013**.
58. M. E. Tuckerman. Ab initio Molecular Dynamics: Basic Concepts, Current Trends and Novel Applications. J. Phys.: Condens. Matter, **2002**, 14, R1297.
59. W. L. Jorgensen, J. Chandrasekhar, J. D. Madura, R. W. Impey, M. L. Klein. Comparison of Simple Potential Functions for Simulating Liquid Water. J. Chem. Phys. , **1983**, 79, 926.
60. J. G. Harris, K. H. Yung. Carbon Dioxide's Liquid-Vapor Coexistence Curve And Critical Properties as Predicted by a Simple Molecular Model. J. Phys. Chem. , **1995**, 99, 12021-12024.
61. W. L. Jorgensen, D. S. Maxwell, J. Tirado-Rives. Development and Testing of the OPLS All-Atom Force Field on Conformational Energetics and Properties of Organic Liquids. J. Am. Chem. Soc. , **1996**, 118, 11225-11236.
62. W. L. Jorgensen. Optimized Intermolecular Potential Functions for Liquid Alcohols. J. Phys. Chem. , **1986**, 90, 1276-1284.
63. W. L. Jorgensen, J. D. Madura, C. J. Swenson. Optimized Intermolecular Potential Functions for Liquid Hydrocarbons. J. Am. Chem. Soc. , **1984**, 106, 6638-6646.

64. W. L. Jorgensen, J. Tirado-Rives. Potential Energy Functions for Atomic-Level Simulations of Water and Organic and Biomolecular Systems. Proc. Natl. Acad. Sci. U.S.A. , **2005**, 102, 6665-6670.
65. B. Hess, C. Kutzner, D. van der Spoel, E. Lindahl. GROMACS 4: Algorithms for Highly Efficient, Load-Balanced, and Scalable Molecular Simulation. J. Chem. Theory Comput. , **2008**, 4, 435-447.
66. S. Nosé. A Unified Formulation of the Constant Temperature Molecular Dynamics Methods. J. Chem. Phys. , **1984**, 81, 511.
67. W. G. Hoover. Canonical Dynamics: Equilibrium Phase-Space Distributions. Phys. Rev. A: At., Mol., Opt. Phys. , **1985**, 31, 1695.
68. M. Parrinello, A. Rahman. Polymorphic Transitions in Single Crystals: A New Molecular Dynamics Method. J. Appl. Phys. , **1981**, 52, 7182-7190.
69. H. J. C. Berendsen, J. P. M. Postma, W. F. van Gunsteren, A. DiNola, J. R. Haak. Molecular Dynamics with Coupling to an External Bath. J. Chem. Phys. , **1984**, 81, 3684.
70. M. P. Allen, D. J. Tildesley. Computer Simulation of Liquids. Oxford University Press: New york. , **1991.**
71. M. Darvas, L. B. Pártay, P. Jedlovszky, G. Horvai. Computer Simulation and ITIM Analysis of the Surface of Water-Methanol Mixtures Containing Traces of Water. J. Mol. Liq. , **2010**, 153, 88-93.
72. J. Grdadolnik, F. Merzel, F. Avbelj. Origin of Hydrophobicity and Enhanced Water Hydrogen Bond Strength Near Purely Hydrophobic Solutes. Proc. Natl. Acad. Sci. U. S. A. , **2017**, 114, 322-327.
73. W. Humphrey, A. Dalke, K. Schulten. VMD: Visual Molecular Dynamics. J. Mol. Graphics, **1996**, 14, 33-38.